

STOCHASTIC FATIGUE DAMAGE ACCUMULATION DUE TO NONLINEAR SHIP LOADS

Alok K. Jha

Bechtel Offshore, Inc.
45 Fremont Street
San Francisco, CA 94105-1895, USA

Steven R. Winterstein

Civil & Environmental Eng. Dept.
Stanford University
Stanford, CA 94305-4020, USA

Abstract

Efficient methods are described here to predict the stochastic accumulation of fatigue damage due to nonlinear ship loads that are produced in random seas. The stochastic analysis method, which may be applied both to overload and fatigue limit states, is based on a relatively new concept: the “nonlinear transfer function” (NTF) method. The basic goal of this method is to require the use of a generally expensive, nonlinear time-domain ship load analysis for only a limited set of idealized, regular waves. This establishes the so-called nonlinear transfer function; i.e., the generally nonlinear transformation from wave amplitude and period to the load amplitude measure of interest (e.g., total load range for rainflow-counting, tensile portion for crack propagation, etc.). Stochastic process theory is used (1) to identify a minimal set of regular waves (i.e., heights and periods) to be applied, (2) to assign an appropriate set of “side-waves” to be spatially distributed along the ship, and (3) to determine how these results should be weighted in predicting statistics of the loads produced in random seas.

The result is compared here with full nonlinear analysis of a specific ship, over long simulations of an irregular sea. A ship with relatively flared cross-section is chosen,

which shows marked nonlinearity and hence asymmetry in its positive and negative (sag and hog) mid-ship bending moment. The NTF method is shown to accurately predict the results of the long nonlinear simulations. This suggests the potential for considerable reduction in analysis costs: time-domain analysis over many cycles of an irregular sea is replaced by a limited number of regular wave analyses.

Introduction

To predict ship loads and resulting responses, there is an ongoing trend toward increasingly detailed, numerically complex analysis methods (e.g., Nakos & Sclavounos, 1990; Lin & Yue, 1990; Kring, 1994; Lin *et al.*, 1994). This increased numerical detail does not come without cost, however. In practice this computational expense may result in a fairly limited “budget” of input wave conditions that can feasibly be analyzed. This constraint may be particularly burdensome when predicting long-run fatigue behavior, which depends on the accumulated effect of many random stress cycles over many steady-state ocean conditions (“seastates”).

We therefore propose a relatively efficient method to estimate long-run fatigue statistics from a limited set of non-

linear time domain analyses. This “nonlinear transfer function” method has previously been suggested to model side-shell ship fatigue (Hansen & Winterstein, 1995), and to predict extreme ship motions (Winterstein, 1991). These previous studies, however, have generally lacked confirmation studies using nonlinear time domain analyses of sufficient length for statistical purposes. We perform such confirmatory analyses here, based on detailed study of wave and ship load statistics over 20 hours of time domain simulation.

The simulation-based studies documented here have resulted in a variety of improvements in the method. These include modification of both the underlying assumptions of Rayleigh-distributed wave heights, and of the Longuet-Higgins distribution of wave periods conditional on their heights. A further extension is the additional study of the appropriate construction of adjacent “side waves,” of particular significance for ship structures.

Fatigue predictions are also made here using a conventional frequency-domain stochastic fatigue analysis. This analysis method assumes a *linear* model of ship behavior. Because nonlinear behavior is generally most severe in rare, large-wave conditions, it is often anticipated that linear models may still suffice to predict average fatigue behavior if not ultimate collapse loads. Notably, it is found here that nonlinear effects can significantly affect even average fatigue behavior, particularly for materials that show relatively steep $S-N$ fatigue curves (i.e., large values of the exponent b that relates stresses to damage).

It should also be noted that while this methodology is proposed and studied here in the context of ship loads, it is intended to be generally applicable to any offshore structure or vessel that responds primarily in a quasi-static (although nonlinear) manner under random wave excitation.

Ship Model

We apply our fatigue analysis procedures to a particular monohull ship. A body plan and a strip model of this ship are shown in Figure 1 and the main particulars of the ship are given in Table 1. The cross-section of the ship changes along its length, with flared cross-sections at the ends of the ship and box cross-sections towards mid-ship (see Fig. 1b). The ship-equipment mass and the ship dead-weight cause nonuniform mass distribution along its length. A ship moving in the waves is subjected to many kinds of loads: vertical and horizontal bending moments, torsional moments, side shell intermittent water pressures, etc. In this study we consider only the mid-ship vertical bending moments (or equivalently, the mid-ship bending stresses) as loads on the ship. The sagging condition causes tensile stresses in the ship bottom, while the hogging condition may extend fatigue cracks in the ship deck. Lateral side shell or torsional

Table 1: Main Particulars of Ship presented in Fig. 1

Specification	Value
Length between perpendiculars	166m
Beam	24.65m
Draft	8.85m
Weight	2×10^5 kN
Waterplane Area	2.84×10^3 sq.m

loads are not considered in this study; however, as noted above the methodology developed here may be applicable for these loads as well.

In the analysis performed here, the ship is assumed to be rigid, and responds to wave loads under head seas in the heave and pitch degrees of freedom. The time-domain nonlinear analysis method used in this study is an in-house program developed at Det Norske Veritas, denoted NV1418 (Børresen, 1981; Frimm, 1991). This is a 2D analysis program, which uses a simple strip theory approach. The response analysis proceeds by simulating a random wave elevation history in time and space, and integrating the spatially distributed water pressure to the exact wetted surface to find the resulting ship forces and motions. This pressure integration to the instantaneous wetted surface, and the flared hull cross-section, contribute primarily to the nonlinearity in the ship loads. While more sophisticated nonlinear analyses are certainly possible, this simple 2D strip theory analysis provides a useful first candidate with which to confirm simpler analytical methods. It reflects, for example, the asymmetry between sag and hog bending moments due to the flared cross-section. In contrast, a linear analysis is based on the assumption of small ship oscillations and, consequently, its predictions of bending moments do not show any asymmetry between sag and hog. A numerical comparison of these linear and nonlinear predictions follows in the next section.

Ship Response: Linear vs Nonlinear Analysis

We compare here the ship response—specifically, its mid-ship bending moment—as predicted from linear and nonlinear analyses. The ship is assumed to be traveling at a speed of 10 knots ($=5.144$ m/s) into a head sea. The input wave is modelled as a Gaussian process with JONSWAP spectrum, whose parameter values are given by the significant wave height $H_s = 5$ m, spectral peak period $T_p = 10$ s, and peakedness factor $\gamma = 3.3$. This spectral peak period corresponds to a wave length that roughly coincides with the length of

the ship. Therefore, this may be a critical seastate in which to accurately estimate ship loads and responses, and it provides a good test of the simplified nonlinear analysis method proposed here.

In the linear analysis, ship loads are estimated by integrating water pressures not to the actual instantaneous surface, but rather to the mean water level (WAVESHIP, 6.1, 1993). This results in a linear transfer function, as shown in Fig. 2, which relates the wave elevation process $\eta(t)$ to the mid-ship bending moment response. Note the peak in this linear transfer function at about $f = 0.1\text{Hz}$. This amplification is again a geometrical effect: it occurs at waves whose lengths coincide with the ship length.

Figure 3 shows a representative portion of the time histories of the waves (as measured at the middle of the ship), and the corresponding mid-ship bending moment predicted by both linear and nonlinear analyses. As expected, the nonlinear analysis is found to yield sag bending moments (positive peaks) that are typically larger than the neighboring hog bending moments (absolute value of negative peaks). This asymmetry is not captured by the linear analysis. Also, as compared with the more accurate nonlinear model, the linear model appears to underestimate the net range (i.e., sag+hog) of the bending moment history. This is significant in that a number of fatigue models use this range as their governing load parameter.

Table 2 shows the corresponding summary statistics of the response, as predicted both by linear and nonlinear analyses. Note that if the bending moment response $x(t)$ has mean value μ , its variance σ^2 is defined as the average value of $[x(t) - \mu]^2$. The corresponding standard deviation (rms) value, σ , provides a useful measure of the average response amplitude. Notably, the linear analysis underestimates σ by roughly 30%; thus, even if a Gaussian model of $x(t)$ is assumed (consistent with a linear analysis), its rms is considerably underestimated by applying the linear ship transfer function. This supports the qualitative observation, from Figure 3, that bending moment ranges tend here to be underestimated by linear theory.

The skewness α_3 and kurtosis α_4 measure deviations from the Gaussian model, and are special cases of the general *standardized* higher moment α_n , defined as the average value of $[(x(t) - \mu)/\sigma]^n$. For odd values of n , positive values of α_n reflect asymmetry. Thus, the significantly positive skewness, $\alpha_3=0.6$, reflects that the asymmetry between sag and hog, qualitatively observed over the time history portion in Figure 3, persists systematically over the entire history.

Figure 4 compares the fatigue damage from the linear analysis to that from the nonlinear analysis. We assume here that fatigue accumulation is modelled either through Miner’s rule, or through a crack propagation model using a

Table 2: Statistics of Ship Load History

	Linear Analysis	Nonlinear Analysis
Mean μ	0	0.21×10^5 kN.m
Sigma σ	1.06×10^5 kN.m	1.36×10^5 kN.m
Skewness α_3	0	0.6
Kurtosis α_4	3.0	3.4

form of the Paris equation. In either case, a mean damage rate \overline{D} can be defined as the reciprocal of the mean fatigue life. As is commonly the case for variable-amplitude loads, this damage rate is taken to be proportional to $\overline{S^b}$, the b -th moment of the governing stress parameter S over the N_{cycles} stress cycles:

$$\overline{D} \propto \overline{S^b} = \frac{1}{N_{\text{cycles}}} \sum_{i=1}^{N_{\text{cycles}}} S_i^b \quad (1)$$

The parameter b here is a material property, reflecting the slope of either the S - N curve ($1/N \propto S^b$), or the Paris equation describing the crack growth rate per cycle ($da/dN \propto S^b$).

For the nonlinear time-domain analysis, the damage rate \overline{D}_{NL} is simply taken as the observed b -th moment, as in Eq. 1, over the N simulated stress cycles. We consider here three separate cases, in which the stresses S_i denote either (1) the sag-induced portion of the stress cycle, (2) the hog-induced of the stress cycle, or (3) the total stress range (i.e., sag+hog). The resulting damage, D_{NL} , will be regarded here as the “exact” damage estimate, which will serve as the point of comparison for simplified damage approximations. The corresponding damage from linear theory is simply

$$\begin{aligned} \overline{D}_{LIN} &\propto \overline{S^b} = \int s^b f(s) ds \\ &= (b/2)! (\sqrt{2}k\sigma)^b \end{aligned} \quad (2)$$

This result uses a Rayleigh model of the probability density $f(s)$. Its result is cast in terms of the rms response σ predicted by linear theory, and the factor k which equals 1 to predict sag or hog stresses, while $k=2$ if the total stress range is to be modelled as the chosen fatigue growth indicator.

Fig. 4 shows that the sag-induced fatigue damage can be considerably underpredicted by the linear model. The linear model more accurately predicts hog-induced damage, as may be anticipated since the hog portions of the predicted bending moments appear closest to those of the nonlinear analysis (see Fig. 3). Note that hog bending moments occur due to wave crests near mid-ship (see Fig. 1) where the cross-section is box-like, suggesting that there is potential

for linear theory to correctly predict hog bending moments. As a net effect of sag and hog, the range-induced fatigue damage is also underpredicted by the linear model, although to a lesser extent than in the case of sag.

As seen in Fig. 4, a nonlinear analysis of sag-induced fatigue for a flared ship can provide larger fatigue damage estimates than a linear analysis, particularly for large values of the fatigue exponent b . We therefore introduce in the next section a new model, which seeks to predict this increased damage due to nonlinear effects, without the expense of full time-domain simulations.

Proposed NTF Model

In the nonlinear transfer function (NTF) model, the major assumption is that the response behavior may be nonlinear but remains essentially memoryless. That is, a single sinusoidal wave cycle of the form $\eta(t)=A \cos(\omega t)$ always gives rise to a regular load/response $x(t)$ with the same frequency, ω , and amplitude, $H_{NL}(A, \omega)$:

$$x(t) = H_{NL}(A, \omega) \cos(\omega t + \phi) \quad (3)$$

The quantity $H_{NL}(A, \omega)$ is referred to here as the nonlinear transfer function. If the system is in fact linear, $H_{NL}(A, \omega)$ is simply $A \cdot |H_{LIN}(\omega)|$ in terms of the linear transfer function $H_{LIN}(\omega)$. More generally, $H_{NL}(A, \omega)$ permits an arbitrary nonlinear trend of response with A , the input wave amplitude. (Note that the assignment of a symmetric cosine function in Eq. 3 is not critical; in general, H_{NL} can be defined as either the positive or negative amplitude, or the total range, of the generally asymmetric response. Note also that in the linear case, the phase shift ϕ in Eq. 3 is typically captured through the relative sizes of the real and imaginary parts of H_{LIN} . This can also be done by defining a complex-valued H_{NL} , but for fatigue calculations these phase shifts are generally not of fundamental importance.)

The nonlinear model then considers the wave $\eta(t)$ at any time as relatively narrow-band, with well-defined local amplitude A —e.g., an envelope value—and corresponding local frequency ω . If we can estimate the joint probability density $f(A, \omega)$ that various (A, ω) pairs will occur within a random seastate, the corresponding average fatigue damage can be estimated as

$$\begin{aligned} \bar{D} \propto \bar{S}^b &= \int_{\text{all } A, \omega} [H_{NL}(A, \omega)]^b f(A, \omega) dA d\omega \\ &\approx \sum_{\text{all } i, j} [H_{NL}(A_i, \omega_j)]^b p_{ij} \end{aligned} \quad (4)$$

In this section we consider appropriate choices of $f(A, \omega)$, based on the observed behavior of our simulated Gaussian

wave histories $\eta(t)$. The following section uses these models, discretized into probabilities p_{ij} of falling into various (A_i, ω_j) cells, to estimate damage as in Eq. 4.

Early applications of the NTF method (e.g., Winterstein, 1991; Hansen & Winterstein, 1995) have used basic models of $f(A, \omega)$, arising from random vibration theory of narrow-band Gaussian processes. The resulting wave amplitudes were assumed to be Rayleigh distributed, and the conditional density $f(\omega|A)$ of frequency given amplitude used the Longuet-Higgins model (Longuet-Higgins, 1983), again based on envelopes of a narrow-band process. Here, however, we propose to replace the Rayleigh distribution for wave amplitude (and height) with a different model proposed by Forristall (Forristall, 1978). This is an empirical distribution, based on measured wave data. Both the Rayleigh and Forristall models are special cases of general Weibull models, which when applied to the wave height H gives results of the form

$$F_H(h) = P[H < h] = 1 - \exp \left[-\frac{(h/\sigma_\eta)^\alpha}{\beta} \right] \quad (5)$$

in which $\sigma_\eta = H_s/4$ is the standard deviation of the wave elevation process $\eta(t)$. For the Rayleigh model $\alpha = 2$ and $\beta = 8$, while the Forristall model uses the slightly altered parameter values $\alpha = 2.126$ and $\beta = 8.42$. (These values of the scale factor, β , should be halved to model the wave amplitude $A=H/2$.) Note that the Rayleigh distribution is a theoretical distribution for a narrow-band Gaussian $\eta(t)$, and to the degree $\eta(t)$ is not narrow-band, the Rayleigh distribution will tend to overestimate wave height fractiles with respect to simulated Gaussian behavior. The Forristall model indeed predicts somewhat lower heights in the upper tail, due mainly to its larger decay rate α . Figure 5 confirms that this Forristall model indeed provides a closer fit than the Rayleigh model to the simulated wave heights in this example seastate (with the JONSWAP spectral parameters $H_s=5\text{m}$, $T_p=10\text{s}$). Similar comparisons of the Forristall model with simulated second-order waves were also found in the wave studies conducted by Jha, 1997a; Jha, 1997c.

For the conditional distribution of wave frequency ω given wave amplitude a , the Longuet-Higgins model suggests a truncated normal distribution:

$$P[\omega > \omega_0] = C \cdot \Phi \left(\frac{\bar{\omega} - \omega_0}{\sigma_{\omega|a}} \right) ; \quad \sigma_{\omega|a} = \frac{\bar{\omega} \Delta}{a/\sigma_\eta} \quad (6)$$

in terms of a mean frequency measure $\bar{\omega}$, a spectral bandwidth parameter Δ , the standard normal distribution function Φ , and the normalizing factor C . $C^{-1} = \Phi(\bar{\omega}/\sigma_{\omega|a})$ to ensure that $P[\omega > 0]=1$. The quantities $\bar{\omega}$ and Δ are commonly defined in terms of the wave spectral moments $\lambda_n = \int \omega^n S_\eta(\omega) d\omega$: $\bar{\omega} = \lambda_1/\lambda_0$ and $\Delta = \sqrt{\lambda_0 \lambda_2 / \lambda_1^2 - 1}$. For

example, $\Delta = 0.42$ for a Pierson-Moskowitz spectrum, and decreases from this value for a JONSWAP spectrum with $\gamma > 1$. Similar models for the conditional distribution have been proposed by Canavie *et al.*, 1976 and Lindgren & Rychlik, 1982; however, these require at least the fourth spectral moment, which is not generally available for wave spectra.

Based on various comparisons with simulated data, we instead assign the mean frequency $\bar{\omega}$ as the value $2\pi/(\cdot.92T_p)$. Figure 6 shows a comparison of the 16th, 50th (median), and 84th percentile values of wave periods T from simulation to this “modified” Longuet-Higgins model. (Note that the corresponding probability $P[T < t_0]$ is equivalent to $P[\omega > 2\pi/t_0]$; the latter is then evaluated from Eq. 6.) For wave heights above about 4 meters, reasonably good agreement is found between the predicted and observed percentiles. For smaller wave heights, the theoretical wave periods exceed the simulated periods; however, there is negligible contribution to fatigue damage from these small-height waves. Thus, from a fatigue damage standpoint, the modified Longuet-Higgins model appears to offer a satisfactory approximation to the conditional distribution of wave periods given a wave height.

Predicted NTF Fatigue Damage vs. Simulated Data

For our baseline NTF prediction, we select 30 sinusoidal waves (see Fig. 7) at which to predict the nonlinear transfer function. (We will return below to consider the sensitivity to the number of waves chosen.) These 30 waves assign 10 equi-spaced wave heights H_i , each with 3 associated periods $T_j|H_i$ located at the 16th, 50th, and 84th percentile values of the modified Longuet-Higgins distribution (see Fig. 6). Discrete probability weights p_{ij} for the 30 pairs have been assigned by discretizing the Forristall distribution of H , and the modified Longuet-Higgins distribution of $T|H$. For example, the three conditional period values $T_j|H_i$ have been assigned equal probability content (the 16th percentile is roughly representative of probability levels from 0 to 1/3, the 50th of levels 1/3 to 2/3, and the 84th of levels above 2/3). Once the transfer function $\overline{H_{NL}}$ has been calculated for these 30 waves, the damage \overline{D}_{NTF} is calculated for different b values as in Eq. 4.

Figure 8 compares the predicted damage from Eq. 4 to the actual damage from the time-domain simulations. This simple implementation of the NTF method somewhat underpredicts the sag-induced damage, by about 25% at $b = 1$, 70% at $b = 4$, and 90% at $b = 10$. This motivates a modification of the method, described below, to better account for adjacent “side” waves. Note, however, that even here the

NTF prediction of sag-induced damage improves upon the linear model, which underpredicts damage by about 90% for $b = 4$ and by almost 2 orders of magnitude at $b = 10$. The predicted hog damage from the NTF method seems here to be in good agreement over the range of b values shown.

Selection of Side Wave Parameters

In the preceding analysis, the nonlinear transfer function H_{NL} was evaluated by applying 30 regular, sinusoidal waves with prescribed heights, H , and periods, T . In a random sea, however, a single wave with height H and period T need not be surrounded by neighboring waves of the same shapes. In particular, a wave with unusually large height is typically surrounded by waves of smaller heights, which regress toward the mean of the underlying wave height distribution. We seek here to quantify this effect, to assign consistent heights and periods, H_0 and T_0 , that are most likely to be associated with a central wave of height H and period T (Fig. 9). These are then applied to each of the 30 (H, T) points used in our NTF prediction, to determine whether the result provides better agreement with full time-domain simulation.

For the 20 hours of simulated Gaussian waves in the given seastate, the empirical relation $E[H_0|H] = 0.46(H/2)^{1.5} + 2$ has been fit directly to the wave height data (Jha, 1997c). This was obtained by pairing every wave height with the height of the next (side) wave in the simulated history. Alternatively, a linear regression model can be directly postulated:

$$E[H_0|H] = m_H + \rho_{H,H_0}(H - m_H) \quad (7)$$

Values of the mean wave height, m_H , and the correlation ρ_{H,H_0} between successive heights, can be estimated by random vibration theory. For example, the Forristall wave height distribution in Eq. 5 has mean value $m_H = 2.4\sigma_\eta$, which for this seastate becomes $m_H = 3.0\text{m}$. Evaluating the correlation function of the wave input, $\rho_\eta(\tau)$, at a lag τ corresponding to an average wave period, results in the correlation estimate $\rho_{H,H_0} = 0.56$. Figure 10 shows that both of these fitted forms capture the simulated trends found in this example seastate. This figure shows the mean and mean \pm 1 standard deviation of H_0 , given various H values in the wave history.

Finally, the period T_0 of the side wave is taken to be the median period from the modified Longuet-Higgins model, based on its corresponding height H_0 . (Given H_0 , we find little additional correlation between T_0 and neighboring period T .) This permits construction of wave triplets for each of the 30 waves chosen in Fig. 7.

NTF prediction using triplets

Recall from Fig. 8 that using sinusoidal waves, NTF damage predictions are somewhat unconservative for sag, while fairly accurate for hog. Figure 11 shows that by instead using wave triplets, the agreement in sag is considerably improved, while the accuracy in hog is fairly well maintained. (Now, hog-induced damage is overpredicted for small b 's by about 30% and underpredicted for large b 's by about 20%.) The net result is rather uniform accuracy, in both sag and hog, over a wide range of b values. This is particularly notable in view of the magnitude of prediction errors that arises from conventional linear models. Figures 12 and 13 illustrate this, comparing directly the linear and NTF predictions (with triplets) for the cases of sag and hog, respectively. It is clear the NTF model provides a considerable improvement, without approaching the cost of full time-domain simulation. (It should be noted that estimation of stresses and the resulting fatigue damage in the NTF model took only about 15 minutes of computer time on an HP 9000 workstation, while generation of 20 hours of simulated stresses took about 6 days on the same computer.)

We next investigate the sensitivity of the NTF prediction to the number of waves chosen. We will limit the choice to 15 waves instead of the 30 selected earlier, but locate these at quadrature points to make best use of these limited resources. Figure 14 shows the locations of the 15 waves chosen. Five wave heights were chosen from the Forristall distribution (Eq. 5) based on Gauss-Laguerre quadrature points, and for every wave height we choose three wave periods based on Gauss-Hermite quadrature points (Winterstein, 1991). Figure 15 shows the resulting sag and hog fatigue damage. As compared with Fig. 11, we find similar accuracy for fairly low stress exponents (e.g., up to b values of 4 or 5). This accuracy tends to deteriorate, however, for higher b values. Because quadrature points are designed to be optimal for low-order polynomial integrands, one may expect that higher b values will require a larger number of points, particularly in the most critical, wave height dimension. Thus, the optimal mesh will generally be problem-specific, depending on the degree of nonlinearity between input (e.g., wave height) and resulting fatigue damage.

Further NTF improvements using calibration

Finally, in the course of diagnosing the potential inaccuracies of the NTF model, a variety of additional modifications have also been considered (Jha, 1997b; Jha, 1997c). These can produce still greater accuracy, but their calibration requires additional information concerning the stress process. (For example, they may require that a limited-duration stress simulation be performed.)

One such modification is to explicitly seek to include the variability in stress level, S , produced by different waves with the same height, H and period T . This can relax the assumption of memoryless loading, by directly reflecting the degree to which there is no unique, deterministic relation between H and S . This effect is quantified here by using data to estimate the coefficient of variation (COV) of S given H and T . Figure 16 shows that by including this scatter, NTF predictions of sag-induced damage are improved for a wide range of S - N exponents. The “without correction” result is the same as the NTF sag prediction shown in Fig. 11 where no calibration to simulated stresses has been done. Similar corrections can improve the hog-induced damage predictions, particularly when a bias factor is also introduced. More details on these and other corrections can be found in Jha, 1997b; Jha, 1997c.

Summary and Conclusions

- A relatively new, “nonlinear transfer function” (NTF) method has been described, and used to predict ship fatigue induced by mid-ship sag and hog bending. The method applies a nonlinear time-domain load analysis at only a limited, critical set of idealized, regular waves. This establishes the nonlinear transfer function; i.e., the generally nonlinear transformation from wave amplitude and period to the load amplitude measure of interest (e.g., total load range for rainflow-counting, tensile portion for crack propagation, etc.).
- To select the critical set of wave heights and associated probability weights, a discretized version of the Forristall wave height distribution has been suggested. A modified version of the Longuet-Higgins model, which rescales the frequency axis to better conform with simulation, has been introduced to select sets of wave periods for each of the given wave heights.
- For spatially distributed ship structures, it is found important to surround the central wave cycle, as characterized by the Forristall and Longuet-Higgins models, not by identical waves but rather with an appropriately modified set of “most likely” side waves. The conditional parameters of the side waves have been proposed here based on probability theory, and shown to match well with the behavior of simulated waves. Using the NTF model with triplets particularly improves its prediction of sag-induced damage, the most severe nonlinear effect found for this flared ship.
- In the example seastate considered for the damage comparisons, the NTF model (with triplets) predicted damage quite close to the results from the full time-domain

simulation, particularly in view of the magnitude of prediction errors that arises from conventional linear models (see Figs. 12 and 13). It is clear that the NTF model provides a considerable improvement, without approaching the cost of full-time domain simulation. Note that the NTF model took only about 15 minutes of computer time while the 20 hours of time domain simulation took about 6 days on an HP 9000 workstation.

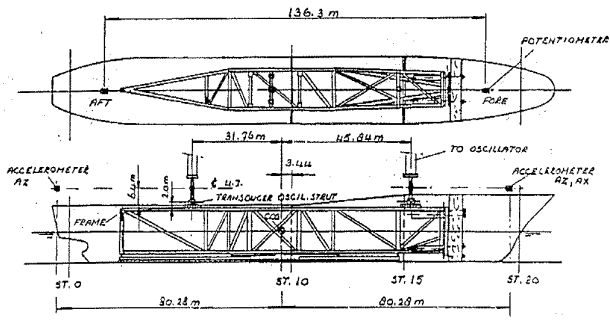
- Further suggested studies include comparison with simulated results across other seastates and over long-term conditions, and for other ship responses. Recall that in an effort to challenge the model's ability to capture nonlinear geometry effects, the seastate used here was chosen to have a characteristic wave length comparable to the ship length.

Acknowledgments

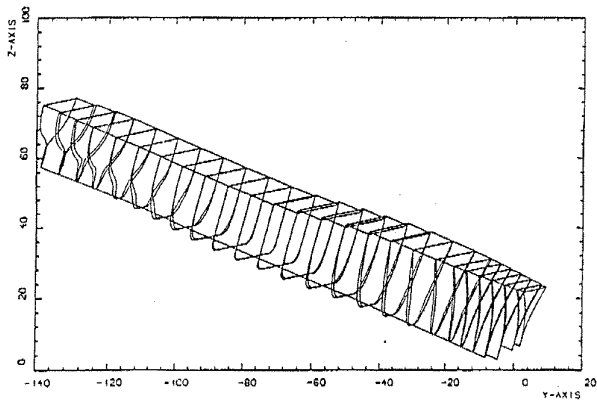
This study is part of the doctoral work of the first author and has been funded by the Office of Naval Research through Grant N00014-9610641. Additional financial support has been provided by the industry sponsors of the Reliability of Marine Structures Program of Stanford University. We thank Det Norske Veritas, Hovik, Norway for donating the numerical ship model and the ship analysis program.

References

- Børresen, T. 1981. *NV1418- Time Domain Solution of Large-amplitude Ship Motions in Head Seas: Users Manual*. Tech. rept. 81-0575. Det Norske Veritas, Oslo, Norway.
- Canavie, A., Arhan, M., & Ezraty, R. 1976. A Statistical Relationship Between Individual Heights and Periods of Storm Waves. *In: Proceedings BOSS'76*, vol. 2.
- Forristall, G. Z. 1978. On the Statistical Distribution of Wave Heights in a Storm. *Journal of Geophysical Research*, **83**(C5), 2353–2358.
- Frimm, F. 1991. *Implementation of Irregular Waves into Program NV1418*. Tech. rept. Veritas Marine Services (U.S.A.), Inc.
- Hansen, P.F., & Winterstein, S.R. 1995. Fatigue damage in the side shells of ships. *Marine Structures*, **8**, 631–655.
- Jha, A. K. 1997a. *Nonlinear Random Ocean Waves: Prediction and Comparison with Data*. Tech. rept. RMS-24. Civil Engr. Dept., Stanford University, Reliability of Marine Structures.
- Jha, A. K. 1997b. *Nonlinear ship loads and ship fatigue reliability*. Tech. rept. RMS-26. Civil Engr. Dept., Stanford University, Reliability of Marine Structures.
- Jha, A. K. 1997c. *Nonlinear stochastic models for loads and responses of offshore structures and vessels*. Ph.D. thesis, Stanford University.
- Kring, D. C. 1994 (May). *Time Domain Ship Motions by a 3-Dimensional Rankine Panel Method*. Ph.D. thesis, Massachusetts Institute of Technology.
- Lin, W. M., & Yue, D. K. P. 1990. Numerical Solutions for Large-Amplitude Ship Motions in the Time Domain. *In: 18th Symposium on Naval Hydrodynamics*. University of Michigan, Ann Arbor, MI, USA.
- Lin, W.-M., Meinhold, M. J., Salvesen, N., & Yue, D. K. P. 1994. Large-Amplitude Motions and Wave Loads for Ship Design. *20th Symposium on Naval Hydrodynamics*, August.
- Lindgren, G., & Rychlik, I. 1982. Wave Characteristic Distributions for Gaussian Waves. *Ocean Engineering*, **9**, 411–432.
- Longuet-Higgins, M. S. 1983 (April). On the Joint Distribution of Wave Periods and Amplitudes in a Random Wave Field. *Pages 241–258 of: Proceedings of the Royal Society of London*.
- Nakos, D. E., & Sclavounos, P. D. 1990. Ship Motions by a Three-Dimensional Rankine Panel Method. *In: Proceedings of the 18th Symposium on Naval Hydrodynamics*.
- WAVESHIP, 6.1. 1993. *Wave Loads on Slender Vessels – Users Manual*. Det Norske Veritas - SESAM, Høvik, Norway.
- Winterstein, S. R. 1991. *Nonlinear Effects of Ship Bending in Random Seas*. Tech. rept. 91-2032. Det Norske Veritas, Oslo, Norway.



(a) Body Plan



(b) Strip Model

Figure 1: Model of monohull ship that will be analyzed using strip theory

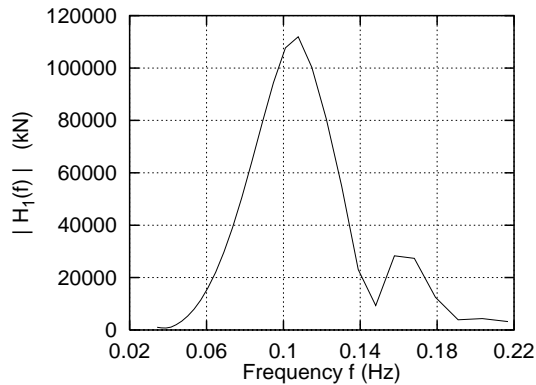
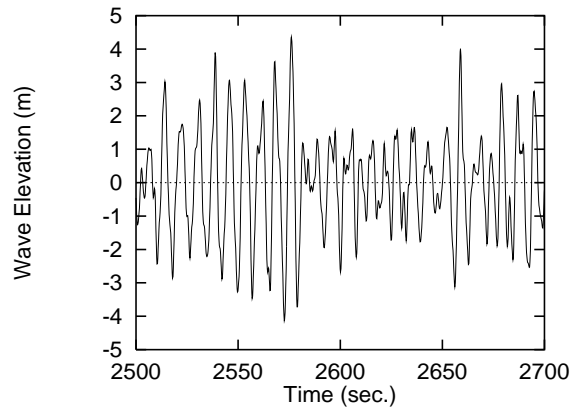
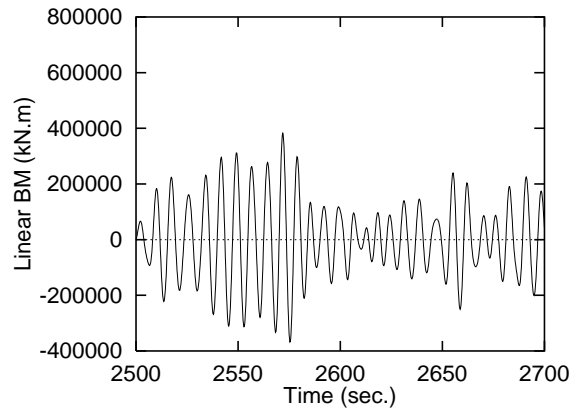


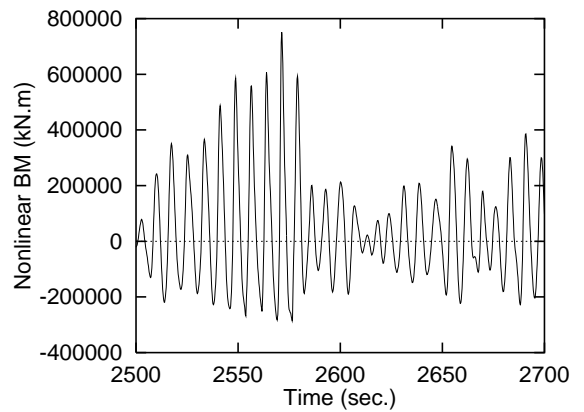
Figure 2: Linear Transfer Function for Mid-ship Bending Moment Response



(a) Wave History



(b) Linear Response History



(c) Nonlinear Response History

Figure 3: Partial wave and response histories at mid-ship

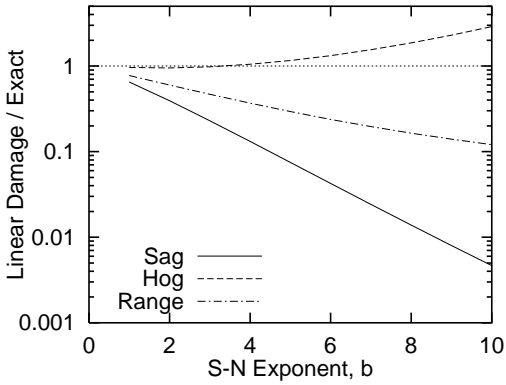


Figure 4: Comparison of fatigue damage from linear and nonlinear analysis for sag, hog and range bending moments

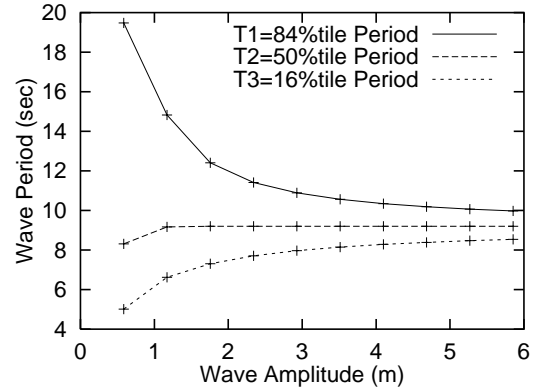


Figure 7: Wave heights and periods for the 30 waves used in the NTF model

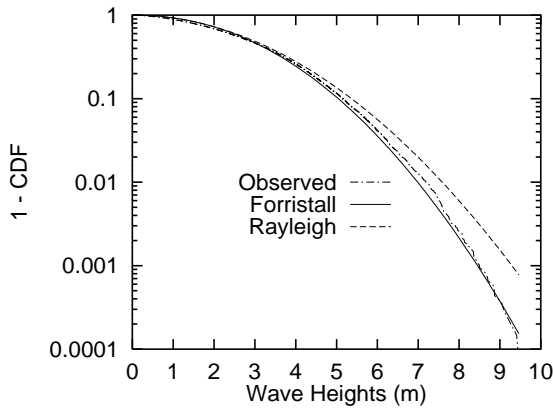


Figure 5: Comparison of simulated wave heights to Forristall and to Rayleigh distributions

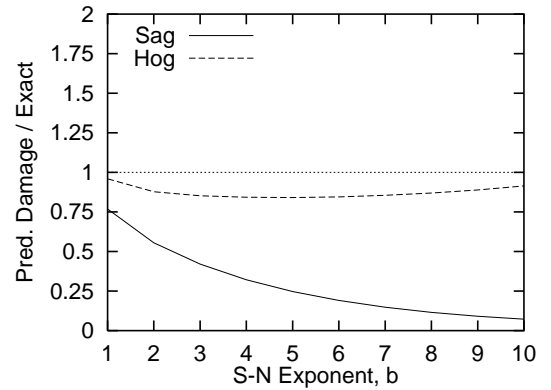


Figure 8: Damage prediction from response to 30 selected sinusoidal waves. The single-wave cycle responses are used in this prediction.

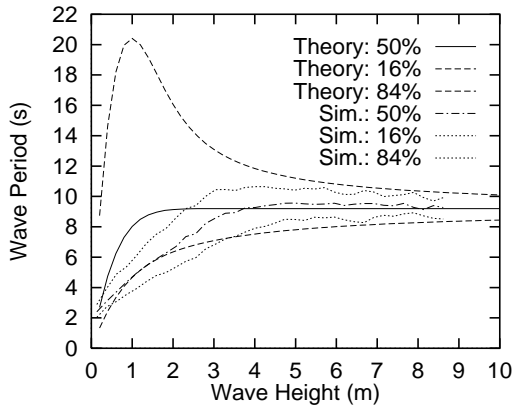


Figure 6: Simulated wave period vs. modified Longuet-Higgins wave period

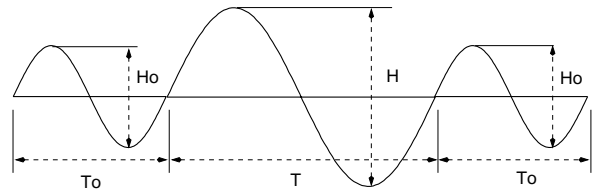


Figure 9: Construction of Wave Triplet for NTF Load Prediction

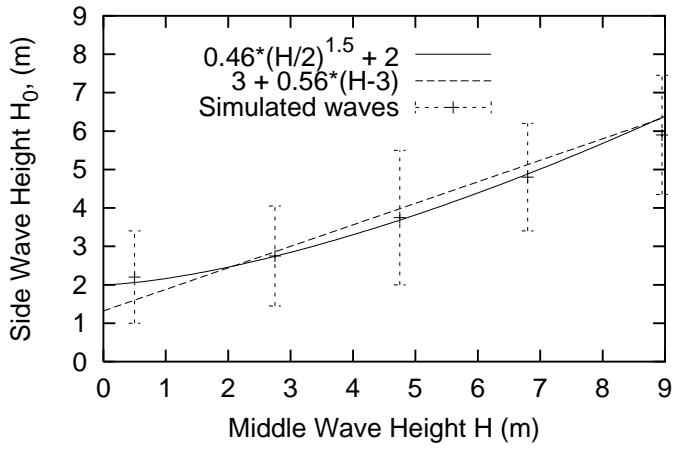


Figure 10: Relation of side wave height to middle wave height

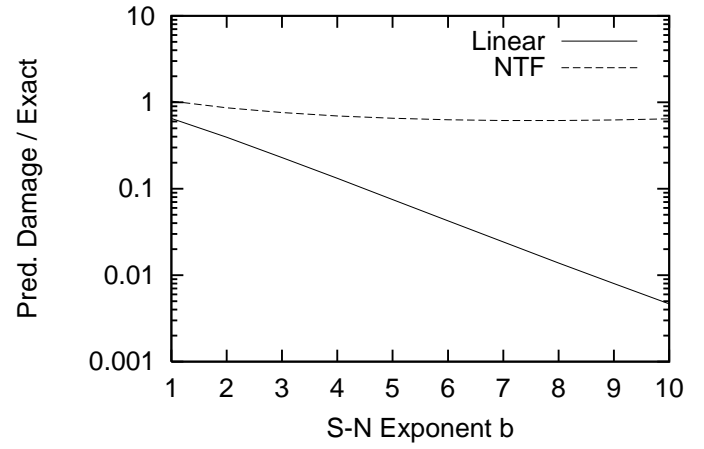


Figure 12: Sag damage prediction from NTF method with 30 triplet waves compared to linear prediction and exact damage

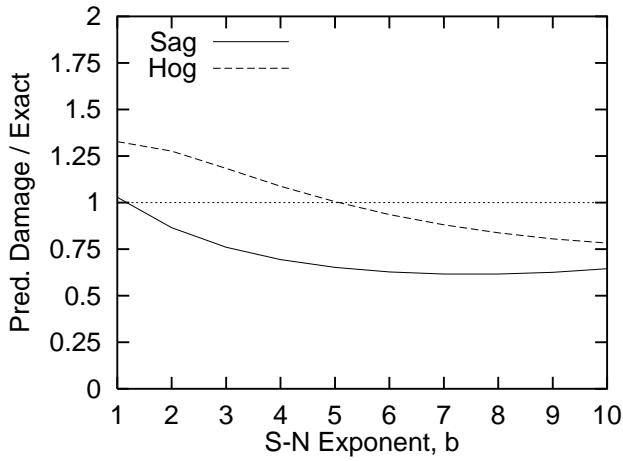


Figure 11: Damage prediction from the response to 30 selected waves as in Fig. 8. Here the side waves have been assigned as “consistent triplets” rather than the regular sinusoids assigned in Fig. 8

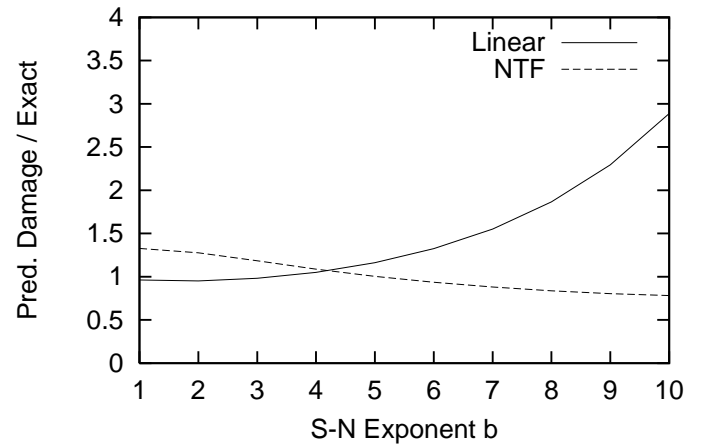


Figure 13: Hog damage prediction from NTF method with 30 triplet waves compared to linear prediction and exact damage

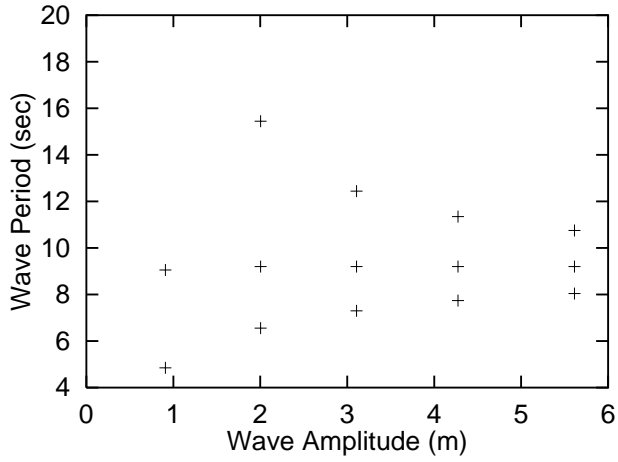


Figure 14: Wave parameters (from quadrature) of the 15 waves in NTF model (Note the largest period for the smallest height not shown, to facilitate comparison with Fig. 7)

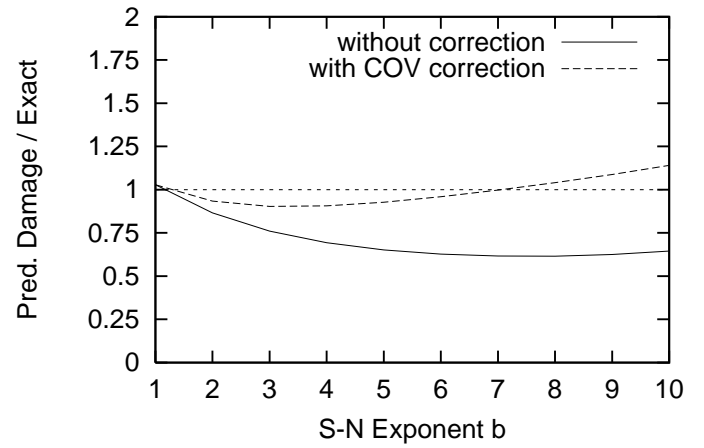


Figure 16: Improvement of NTF prediction for sag damage by including scatter effects

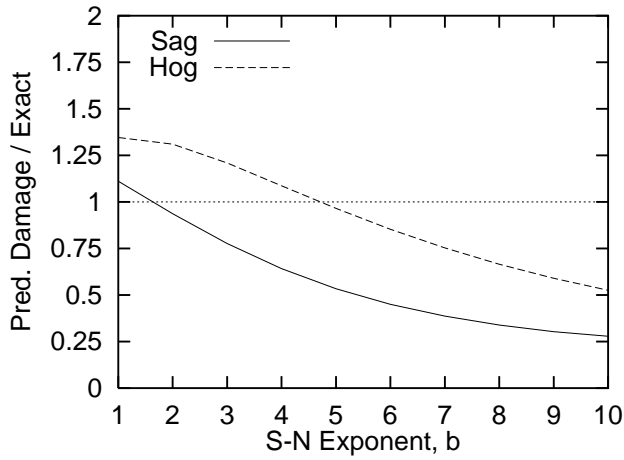


Figure 15: Damage prediction from response to selected waves with side waves. 15 wave triplets have been used in the fatigue prediction.